研究成果の刊行に関する一覧表(書籍)

著者氏名	論文タイトル名	書籍全体の編集者名	書籍名	出版名
原　寿郎	免疫疾患	内山　聖、原　寿郎、高橋孝雄	標準小児科学	医学書院
原　寿郎	全身性自己免疫疾患-自己炎症性症候群	松島綱治、西脇　徹	炎症・再生医学事典	朝倉書店
原　寿郎	原発性免疫不全症：新しい診断、治療法	水谷修紀	第51回日本小児血液学会教育セッションテキスト	小児血液学

Ⅴ．研究成果の刊行物・印刷物

ARTHRITIS & RHEUMATISM
Vol. 60, No. 1, January 2009, pp 242–250
DOI 10.1002/art.24134

Role of the *NOD2* Genotype in the Clinical Phenotype of Blau Syndrome and Early-Onset Sarcoidosis

Ikuo Okafuji,[1] Ryuta Nishikomori,[1] Nobuo Kanazawa,[2] Naotomo Kambe,[3] Akihiro Fujisawa,[1] Shin Yamazaki,[1] Megumu Saito,[1] Takakazu Yoshioka,[1] Tomoki Kawai,[1] Hidemasa Sakai,[1] Hideaki Tanizaki,[1] Toshio Heike,[1] Yoshiki Miyachi,[1] and Tatsutoshi Nakahata[1]

Objective. **Blau syndrome and its sporadic counterpart, early-onset sarcoidosis (EOS), share a phenotype featuring the symptom triad of skin rash, arthritis, and uveitis. This systemic inflammatory granulomatosis is associated with mutations in the *NOD2* gene. The aim of this study was to describe the clinical manifestations of Blau syndrome/EOS in Japanese patients and to determine whether the *NOD2* genotype and its associated basal NF-κB activity predict the Blau syndrome/EOS clinical phenotype.**

Methods. **Twenty Japanese patients with Blau syndrome/EOS and *NOD2* mutations were recruited. Mutated *NOD2* was categorized based on its basal NF-κB activity, which was defined as the ratio of NF-κB activity without a *NOD2* ligand, muramyldipeptide, to NF-κB activity with muramyldipeptide.**

Results. **All 9 mutations, including E383G, a novel mutation that was identified in 20 patients with Blau syndrome/EOS, were detected in the centrally located NOD region and were associated with ligand-independent NF-κB activation. The median age of the patients at disease onset was 14 months, although in 2 patients in Blau syndrome families (with mutations R334W and E383G, respectively) the age at onset was 5 years or older. Most patients with Blau syndrome/EOS had the triad of skin, joint, and ocular symptoms, the onset of which was in this order. Clinical manifestations varied even among familial cases and patients with the same mutations. There was no clear relationship between the clinical phenotype and basal NF-κB activity due to mutated *NOD2*. However, when attention was focused on the 2 most frequent mutations, R334W and R334Q, R334W tended to cause more obvious visual impairment.**

Conclusion. ***NOD2*** **genotyping may help predict disease progression in patients with Blau syndrome/EOS.**

Sarcoidosis is a systemic inflammatory disease with unknown etiology, but it can be clinically characterized by swelling of the bilateral hilar lymph nodes and histologically defined by the presence of noncaseating epithelioid cell granulomas. A special subtype called early-onset sarcoidosis (EOS; MIM no. 609464) occurs in children younger than 4 years of age and is characterized by a distinct triad of skin, joint, and eye disorders without apparent pulmonary involvement (1). An autosomal-dominant disease with clinical manifestations similar to those of EOS has been recognized as Blau syndrome (MIM no. 186580) (2,3). The gene responsible for Blau syndrome has been mapped close to the inflammatory bowel disease 1 (*IBD1*) locus by linkage analysis (4), and later the nucleotide-binding oligomerization domain 2 gene (*NOD2*) was identified by Miceli-Richard et al to be responsible for Blau syndrome (5). In the study by Miceli-Richard et al, 2 European patients with EOS had no mutation in *NOD2*; therefore, it remained

Supported by the Ministry of Education, Science, Sports, and Culture, Japan.

[1]Ikuo Okafuji, MD, Ryuta Nishikomori, MD, PhD, Akihiro Fujisawa, MD, PhD, Shin Yamazaki, PhD, Megumu Saito, MD, PhD, Takakazu Yoshioka, MD, Tomoki Kawai, MD, Hidemasa Sakai, MD, Hideaki Tanizaki, MD, Toshio Heike, MD, PhD, Yoshiki Miyachi, MD, PhD, Tatsutoshi Nakahata, MD, PhD: Kyoto University Graduate School of Medicine, Kyoto, Japan; [2]Nobuo Kanazawa, MD, PhD: Kyoto University Graduate School of Medicine, Kyoto, and Wakayama Medical University, Wakayama, Japan; [3]Naotomo Kambe, MD, PhD: Kyoto University Graduate School of Medicine, Kyoto, and Chiba University Graduate School of Medicine, Chiba, Japan.

Address correspondence and reprint requests to Ryuta Nishikomori, MD, PhD, Department of Pediatrics, Kyoto University Graduate School of Medicine, 54 Kawahara-cho, Shogoin, Sakyo-ku, Kyoto 606-8507, Japan. E-mail: rnishiko@kuhp.kyoto-u.ac.jp.

Submitted for publication March 19, 2008; accepted in revised form September 5, 2008.

controversial whether Blau syndrome and EOS have the same etiology.

In 2004, we encountered a 27-year-old Japanese man with multiple lichenoid papules. He was almost blind, exhibited camptodactyly, and had a continuous low-grade fever. This case of sporadic systemic granulomatosis with clinical features of EOS showed the same *NOD2* mutation, the arginine-to-tryptophan substitution at amino acid 334 (R334W), as that detected in Blau syndrome (6). Therefore, we expanded this report (6) and retrospectively examined cases of EOS in Japan and observed that 9 of 10 patients with EOS had *NOD2* mutations (7). Until recently, other investigators have also confirmed that Blau syndrome and EOS are clinically and genetically identical across various ethnic groups (8–10).

NOD2 activates NF-κB after recognizing a signal from a bacterial cell wall component, muramyldipeptide, in the cytoplasm of monocytes, and thus can work as an intracellular sensor of bacteria (11,12). *NOD2* has a tripartite domain structure consisting of 2 amino-terminal domains (termed caspase activation and recruitment domains) that are composed of protein–protein interaction cassettes, 1 centrally located NOD, and carboxy-terminal leucine-rich repeats (LRRs) (13). Using assays of NF-κB activity, an impaired ligand-dependent response was demonstrated for 3 Crohn's disease–associated mutations located in *NOD2* LRRs (14,15), whereas enhanced ligand-independent NF-κB activity was demonstrated for *NOD2* alleles associated with Blau syndrome and EOS (5,7,16). However, it remains unknown how increased basal NF-κB activity derived from gain-of-function mutations in *NOD2* affects the pathogenesis of Blau syndrome/EOS and whether a genotype–phenotype correlation exists between the clinical manifestations or onset of Blau syndrome/EOS and *NOD2* mutations.

Because Blau syndrome/EOS is so rare, very few reports are in the literature. Therefore, it was worthwhile to conduct a nationwide survey limited to patients with a specific ethnic background, such as Japanese patients. In this study, we precisely documented the clinical manifestations in a cohort of Japanese patients with Blau syndrome/EOS and *NOD2* mutations, including 9 previously reported cases (7), and explored the genotype–phenotype correlation to the basal NF-κB activity associated with each mutation, especially focusing on the correlation of visual impairment with the most frequent mutations, R334W and R334Q.

PATIENTS AND METHODS

Patients and clinical information. Among patients with clinically diagnosed Blau syndrome/EOS, the 20 patients with *NOD2* mutations were included in this study (7,17–20). None of these mutations were identical to the reported single-nucleotide polymorphisms (SNPs) of *NOD2*, nor were they detected in 100 Japanese healthy volunteers. Clinical information and patient histories were collected from medical records and by direct interviews of the patients and their attending physicians. The presence of each symptom was established as follows: a) persistent or repeated transient skin lesions without definite cause were determined, b) persistent or repeated transient arthritis without definite cause was determined, c) uveitis was diagnosed by an ophthalmologist, and d) remittent or intermittent fever without definite cause was determined under close examination at the time of hospital admission. The age at disease onset was defined as the age of the patient when any of the above-mentioned symptoms appeared.

Clinical evaluation was performed primarily when individual symptoms first appeared that were hardly affected by treatment or disease duration. The severity of visual impairment was assessed in accordance with the World Health Organization definition (21). Briefly, moderate visual impairment was defined as visual acuity between 6/18 and 3/60, and severe visual impairment was defined as acuity of 3/60 or less in the better eye with best correction, as previously described (9). Written informed consent was obtained from the patients and their families, and the study protocol was in accordance with the guidelines of the Institutional Review Board of Kyoto University Hospital.

Genetics analysis. Genomic DNA was extracted from the peripheral blood of the patients, and sequencing of all exons and exon–intron junctions of *NOD2* was performed as previously described (7).

Generation of *NOD2* mutants and NF-κB luciferase assay. Expression plasmids of *NOD2* and its mutants were subcloned into the p3xFLAG-CMV vector, as previously described (7). Blau syndrome/EOS–associated mutants were generated using the QuikChange site-directed mutagenesis kit (Stratagene, La Jolla, CA), as described previously (7). The ability of each construct to induce NF-κB activity was assessed by dual luciferase reporter assay in HEK 293 human embryonic kidney cells, as previously described (7).

Other analyses. We determined the age at the time of this survey, the age at onset of each symptom, and the *NOD2* genotype for all patients as well as the distribution of age at disease onset. Next, we analyzed the relationship between age at disease/symptom onset and basal NF-κB activity due to mutated *NOD2*. Basal NF-κB activity was defined as the ratio of NF-κB reporter activity without muramyldipeptide to NF-κB reporter activity with muramyldipeptide, as determined using the in vitro NF-κB luciferase assay described above. The activity was arbitrarily categorized as low (<0.3), moderate (0.3–0.5), and high (>0.5). Finally, we analyzed the relationship between visual impairment (normal, moderate, severe) and basal NF-κB activity (low, moderate, high) due to individual mutated *NOD2* genes, particularly the 2 most frequent mutations, R334W and R334Q. We did not perform statistical analysis because of the limited number of patients.

Table 1. Demographic and clinical characteristics of the patients with Blau syndrome/early-onset sarcoidosis*

Patient/ age/sex	Genotype	Fever		Skin rash		Arthritis		Uveitis		Visual acuity		Ref.
		Age at onset	Type	Age at onset	Type	Age at onset	Type	Age at onset	Type	OD	OS	
1/15/F†	E383G	2 yr 3 mo	Int	8 mo	LP/SE/EN	3 yr	Poly	11 yr	A/P	20/50	20/67	
2/48/F†	E383G	5 yr	Per	5 yr	LP/SE/EN	11 yr	Poly	11 yr	A/P	HM	Null	
3/36/F	H496L	–	–	1 yr	LP/SE	3 yr	Poly	5 yr	A/P	20/20	20/20	7
4/16/M	R334Q	1 yr 8 mo	Int	6 mo	LP/SE	1 yr 8 mo	Poly	1 yr 10 mo	A/P	20/22	20/22	
5/19/M	R334Q	2 yr 7 mo	Per	1 yr 4 mo	LP/SE/EN	10 mo	Poly	5 yr	A/P	20/50	20/20	17
6/8/F	R334Q	–	–	–	–	3 yr	Poly	–	–	20/20	20/20	
7/8/M	T605P	–	–	7 mo	LP/SE	1 yr 6 mo	Poly	3 yr 3 mo	A/P	20/25	20/50	7
8/18/F	D382E	–	–	3 yr 4 mo	LP/SE	4 yr	Poly	5 yr 4 mo	A/P	20/20	20/25	7, 18
9/13/M	R334W	8 mo	Per	1 yr 3 mo	LP/SE/EN	8 mo	Poly	1 yr 8 mo	A/P	20/29	20/33	
10/32/M	R334W	2 yr	Int	2 yr	LP/SE	1 yr 3 mo	Poly	6 yr	A/P	Blind, 20 yr	Blind, 20 yr	6, 7
11/21/F	R334W	2 yr 1 mo	Per	2 yr 1 mo	LP/SE	6 yr	Poly	4 yr	A/P	20/670	20/330	7, 19
12/33/M	R334W	–	–	2 yr	LP/SE	–	–	13 yr	A/P	20/29	20/20	7
13/31/F	R334W	–	–	2 yr 6 mo	LP/SE	8 yr	Poly	3 yr 6 mo	A/P	20/100	20/200	7
14/10/F†	R334W	1 yr	Per	1 yr	LP/SE	1 yr	Poly	2 yr	A/P	20/40	Null	
15/46/F†	R334W	–	–	44 yr	LP/SE	8 yr	Poly	3 yr	A/P	Blind, 28 yr	Blind, 28 yr	
16/16/M†	R334W	–	–	6 yr	SE	1 yr	Oligo	6 yr	A/P	20/13	20/13	20
17/18/F†	R334W	–	–	12 yr	SE	8 yr	Oligo	12 yr	A/P	20/40	20/25	20
18/8/M	M513T	2 yr 10 mo	Int	2 yr 8 mo	SE	2 yr 9 mo	Poly	2 yr 11 mo	A	20/17	20/17	7
19/15/F	N670K	1 yr 8 mo	Int	5 mo	LP/SE/EN	1 yr 8 mo	Poly	3 yr	A/P	20/200	20/200	7
20/7/M	C495Y	1 yr	Int	1 yr	LP/SE	1 yr	Poly	–		20/20	20/20	

* Patient 5 also had left ventricular dysfunction and pulmonary hemorrhage due to bronchial granuloma. Patient 10 also had interstitial pneumonia. Patient 11 also had hepatosplenomegaly and parotid swelling. Patient 18 also had renal calcification. OD = right eye; OS = left eye; yr = years; mo = months; Int = intermittent; LP = multiple lichenoid papules; SE = scaly erythematous plaques; EN = erythema nodosum–like lesion; Poly = polyarticular; A = anterior; P = posterior; Per = persistent; HM = hand motion; Oligo = oligoarticular.
† Familial case.

RESULTS

Genotype and basal NF-κB activity. The study population comprised 9 male patients and 11 female patients, with a median age of 17 years (range 7–48 years) and a median disease duration of 15 years (range 5–43 years). Fourteen of these 20 cases were sporadic (EOS), and 6 were familial (Blau syndrome). The familial cases were in 3 unrelated families; 2 families (patients 14 and 15 and patients 16 and 17, respectively) had Blau syndrome/EOS symptoms in 2 generations, and 1 family (patients 1 and 2) had Blau syndrome/EOS symptoms in 3 generations. The most frequent heterozygous mutation of *NOD2* was R334W (1000C>T), which was recognized in 2 familial and 5 sporadic cases (total of 9 cases), followed by R334Q (1001G>A) in 3 sporadic cases, and E383G (1148A>G, a novel amino acid substitution) in 2 familial cases (in 1 family). H496L (1487A>T), T605P (1813A>C), D382E (1146C>G), M513T (1538T>C), N670K (2010C>A), and C495Y (1484G>A) were detected in 1 sporadic case each (Table 1).

Nine mutations were identified in the centrally located NOD region (Figure 1a) and were associated with increased basal NF-κB activity in the absence of muramyldipeptide (Figure 1b), which is consistent with the finding of a previous study on Blau syndrome/EOS–associated *NOD2* mutations (16). We also confirmed that 100 healthy control subjects and their genotyped asymptomatic relatives did not have these amino acid substitutions. Therefore, we concluded that these *NOD2* mutations (amino acid substitutions) detected in patients with Blau syndrome/EOS were not SNPs but rather were disease-causing mutations.

Disease onset. The defining characteristic of EOS is its onset in children younger than age 4 years (1). In the present study, despite the median age at disease onset of 14 months, the first clinical symptoms developed at age 5 years or older in 2 patients (patients 2 and 17, who were members of different Blau syndrome families) with the E383G mutation and the R334W mutation, respectively (Table 2). In patient 2, skin rash developed at age 5 years; in patient 17, arthritis developed at age 8 years (Table 1).

The earliest presenting symptom was skin rash in 13 patients (65%), arthritis in 8 patients (40%), and ocular symptoms in 1 patient (patient 15, who had familial Blau syndrome with the R334W mutation) (Table 1). Approximately 95%, 95%, and 90% of pa-

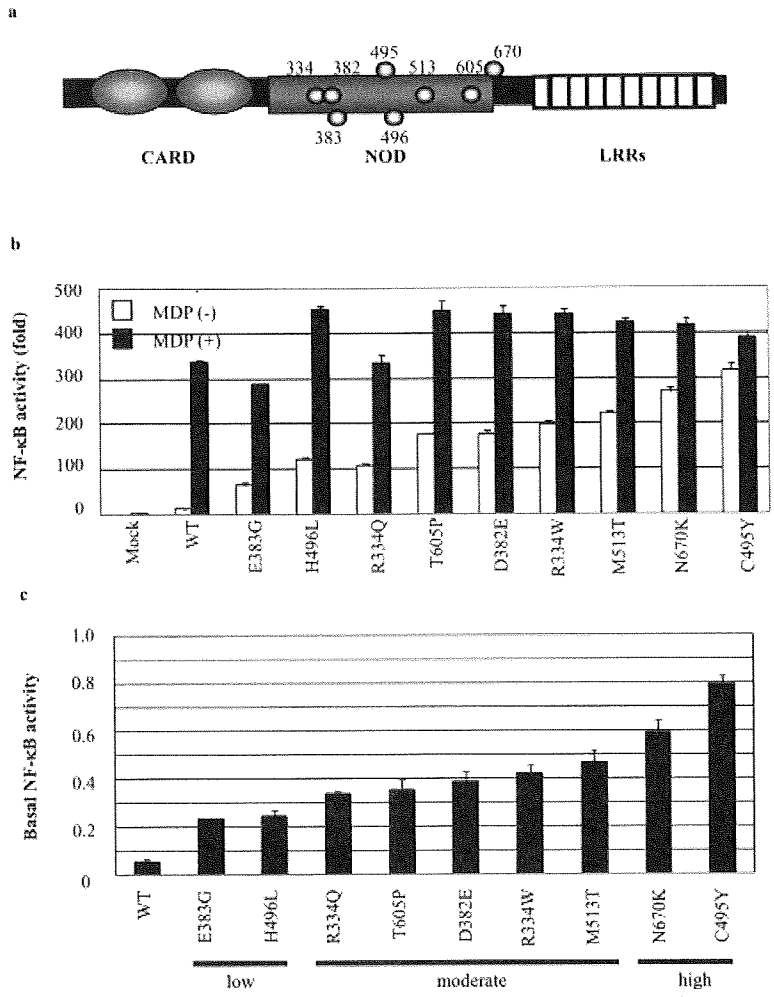

Figure 1. Biologic effects of *NOD2* mutants discovered in patients with Blau syndrome/early-onset sarcoidosis (EOS). **a,** Schematic presentation of NOD-2 protein. Numbers indicate the positions of mutated amino acid residues identified in our cohort. **b,** Increased basal NF-κB activity due to different mutated *NOD2* genes in patients with Blau syndrome/EOS. HEK 293T cells were cotransfected with a *NOD2* mutant together with the NF-κB reporter plasmid and internal control plasmid, and NF-κB reporter activity was measured after 12 hours of incubation with or without muramyldipeptide (MDP; 5 μg/ml). Mock vector and wild-type (WT) *NOD2* were used as controls. Bars show the mean and SD of normalized data (mock without muramyldipeptide = 1) from triplicate cultures. Results are representative of 3 independent experiments. **c,** Basal NF-κB activity due to mutated *NOD2* in patients with Blau syndrome/EOS. Bars show the mean and SD results from 3 independent experiments. CARD = caspase activation and recruitment domain; LRRs = leucine-rich repeats.

tients, respectively, had skin, joint, and ocular symptoms. Consistent with the previous report (1), a triad of skin, joint, and ocular symptoms developed (in this order) in many patients with Blau syndrome/EOS. The median age at onset of rash, arthritis, and uveitis was 24 months, 33 months, and 4.5 years, respectively (Table 2).

The triad of symptoms. All except 1 patient (patient 6 [with the R334Q mutation]) had skin manifestations. Consistent with a previous report (22), the most frequent skin symptom was scaly erythematous plaques with multiple lichenoid papules. Several patients (patients 1 and 2 with the E383G mutation, patient 5

Table 2. Age of the patients at the onset of disease and symptoms*

Age, years	Disease onset (n = 20)	Symptom onset			
		Fever (n = 11)	Rash (n = 19)	Arthritis (n = 19)	Uveitis (n = 18)
0	6 (30)	1 (9)	4 (21)	2 (11)	0 (0)
1	5 (25)	4 (36)	5 (26)	7 (37)	2 (11)
2	4 (20)	5 (45)	5 (26)	1 (5)	2 (11)
3	3 (15)	0 (0)	1 (5)	3 (16)	4 (22)
4	0 (0)	0 (0)	0 (0)	1 (5)	1 (6)
≥5	2 (10)	1 (9)	4 (21)	5 (26)	8 (44)

* Values are the number (%). The median age at disease onset was 1 year 2 months; the median age at onset of fever and rash was 2 years; the median age at onset of arthritis was 2 years 9 months; the median age at onset of uveitis was 4 years 6 months.

with the R334Q mutation, patient 9 with the R334W mutation, and patient 19 with the N670K mutation) had erythema nodosum–like lesions on their lower limbs in addition to solid lichenoid eruptions. Notably, 3 patients (patients 16 and 17 with the R334W mutation and patient 18 with the M513T mutation) showed only scaly erythematous plaques without lichenoid papules (Table 1).

All except 1 patient (patient 12 with the R334W mutation) had joint lesions (polyarticular arthritis in 17 patients and oligoarticular arthritis in 2 [patients 16 and 17]) (Table 1). Both patients with oligoarticular arthritis, who had familial Blau syndrome with the R334W mutation, had camptodactyly without obvious synovial cysts. Camptodactyly with synovial cysts is frequently described as a typical joint sign in patients with Blau syndrome/EOS (10). A consequence of arthritis was the use of a wheelchair for daily mobility in 2 patients (patient 5 with the R334Q mutation and patient 10 with the R334W mutation).

All except 2 patients (patient 6 with the R334Q mutation who also lacked skin eruptions and patient 20 with the C495Y mutation) had ocular lesions. The lesions were bilateral, although visual acuity was asymmetric, as in previous studies (22,23). Moreover, 17 (89%) of all 18 patients with ocular lesions had panuveitis, while only 1 patient (patient 18 with mutation M513T) had anterior uveitis, which demonstrated the predominance of panuveitis over anterior uveitis. Ocular symptoms were the last of the triad to develop in 15 of the 18 patients and the first to develop in only 1 patient (patient 15 with mutation R334W).

Clinical features other than the triad of symptoms. It is noteworthy that 11 patients (55%) experienced fever at a median age of 24 months, almost simultaneously with skin and/or joint symptoms (Table 1). Five patients had persistent fever reaching 38–40°C, and 6 patients had intermittent fever. In particular, in 1 patient (patient 9 with mutation R334W) the disease developed with intermittent fever (which then became persistent fever over the next 6 months) and finger joint swelling. In only 1 previous report (10), fever is mentioned as a clinical symptom of Blau syndrome/EOS, although there are some case reports in which fever was present at disease onset (24).

Four patients had involvement of organs other than the skin, joints, and eyes (Table 1). Two patients had pulmonary lesions (interstitial pneumonitis in patient 10 with the R334W mutation and bronchial granuloma in patient 5 with the R334Q mutation). Bilateral hilar lymph nodes, which are identified by chest radiography and/or computed tomographic scanning, were not observed in any patient. Patient 11 with the R334W mutation exhibited hepatosplenomegaly and parotid swelling (19), and patient 18 with the M513T mutation exhibited renal calcification. No cases of large-vessel vasculitis were observed in this cohort, even though vasculitis has been reported in patients with EOS (25–27).

Triggering factors. BCG vaccination was associated with the onset of disease (i.e., development of multiple papules on the extremities) in 2 patients, although no apparent infection or vaccination was clearly documented in other patients of our cohort. In 1 patient (patient 7 with mutation T605P) who had papules on the extremities, the spread of papules was from the site of BCG vaccination. In the other patient (patient 1 with mutation E383G), Gianotti disease was initially diagnosed, but a close review of her medical history later indicated that her multiple papules were a symptom of Blau syndrome/EOS.

Relationship between the onset of disease/symptoms and basal NF-κB activity due to mutated *NOD2*. Because disease duration and treatment varied among patients, we focused on the onset of disease and of each clinical symptom (i.e., fever, rash, arthritis, and uveitis). We evaluated the relationship between age at the onset of disease/symptoms and basal NF-κB activity due to mutated *NOD2* (defined as the ratio of NF-κB activity without a *NOD2* ligand, muramyldipeptide, to NF-κB activity with muramyldipeptide for each mutated *NOD2*). The calculated basal NF-κB activity ranged from 0.23 to 0.79 (mean 0.42) for mutated *NOD2* and was 0.05 for wild-type *NOD2* (Figure 1c).

Because the number of patients with each *NOD2* mutation was limited, we arbitrarily categorized basal NF-κB activity as low (<0.3), moderate (0.3–0.5), and high (>0.5). According to these criteria, mutations E383G and H496L were associated with low activity; mutations R334Q, T605P, D382E, R334W, and M513T were associated with moderate activity; and mutations

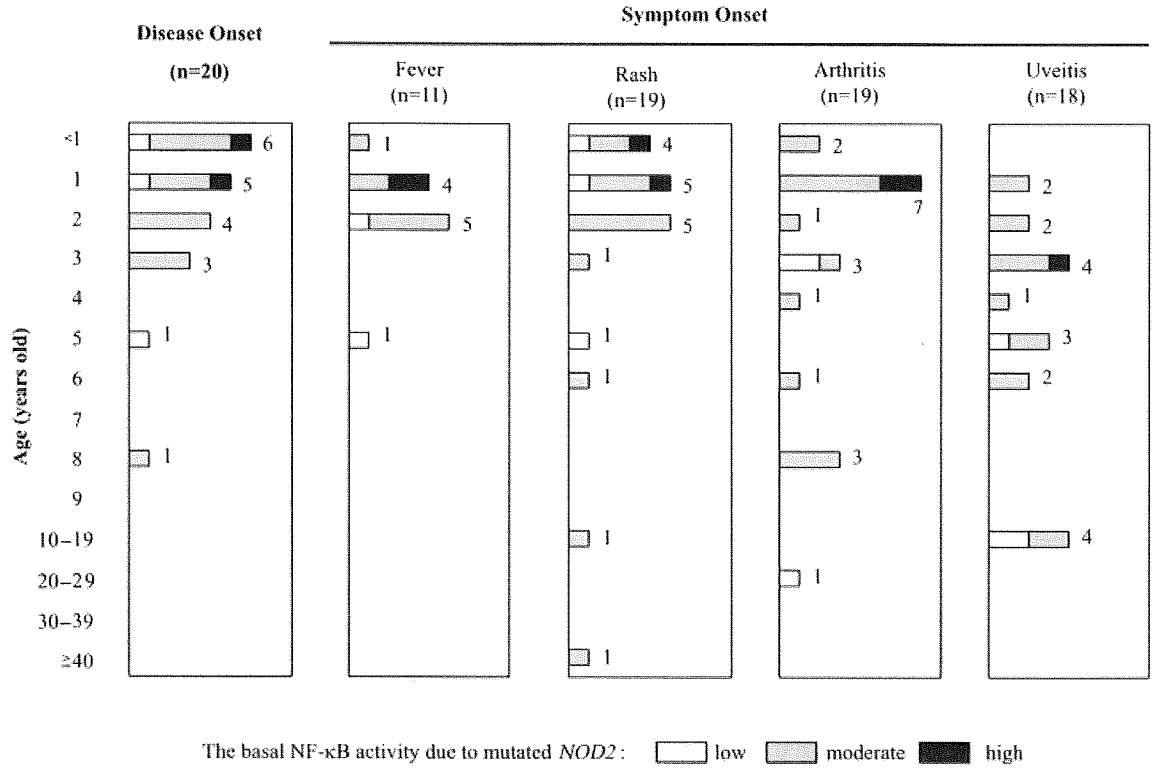

Figure 2. Relationship between age at disease or symptom onset and basal NF-κB activity due to mutated *NOD2*. Among the 9 patients without fever, 8 had moderate and 1 had low basal NF-κB activity. One patient without rash had moderate basal NF-κB activity, and 1 patient without arthritis had moderate basal NF-κB activity. Of 2 patients without uveitis, 1 had high and the other had moderate basal NF-κB activity.

N670K and C495Y were associated with high basal NF-κB activity. Our limited number of patients was insufficient to detect a correlation between the defined basal NF-κB activity and the onset of disease, fever, rash, arthritis, and uveitis (Figure 2). Notably, the age at onset of symptoms varied markedly between patients with the same R334W mutation, even in familial cases (Table 1).

Relationship between visual impairment and basal NF-κB activity due to mutated *NOD2*. The most relevant morbidity associated with Blau syndrome/EOS is ocular involvement, which is usually refractory to conventional treatment. Thus, we next explored the relationship between visual impairment and basal NF-κB activity. There was no clear correlation when the analysis included all recruited patients (Table 3). When we focused on the most frequent genotypes R334Q and R334W, between-genotype differences in visual impairment were observed (Table 4). Basal NF-κB activity was higher in patients with the R334W mutation than in those with the R334Q mutation (Figure 1c). None of the 3 patients with the R334Q mutation had visual impairments, while 4 of 9 patients with the R334W mutation

Table 3. Correlation between visual impairment and basal NF-κB activity*

	Visual impairment			Disease duration, median (range) years
	Normal	Moderate	Severe	
Basal NF-κB activity				
Low	2	0	1	35 (15–43)
Moderate	11	2	2	15 (5–43)
High	1	1	0	10.5 (6–15)

* Except where indicated otherwise, values are the number of patients.

Table 4. Correlation between visual impairment and the 2 most frequent genotypes*

	Visual impairment			Disease duration, median (range) years
	Normal	Moderate	Severe	
Present study				
R334Q	3	0	0	15 (5–19)
R334W	5	2	2	19 (9–43)
Previous study (9)				
R334Q	8	0	0	12 (3–26)
R334W	8	2	1	16 (5–44)

* Except where indicated otherwise, values are the number of patients.

had visual impairments. This result suggests that patients with the R334W mutation were more likely to have visual impairments than were those with the R334Q mutation (Table 4).

DISCUSSION

Blau syndrome/EOS is a rare systemic granulomatosis that has been associated with *NOD2*. In this study, patients with Blau syndrome/EOS and *NOD2* mutations were retrospectively recruited nationwide in Japan, to determine whether the *NOD2* genotype and its functional abnormality predict the Blau syndrome/EOS clinical phenotype. This study is the first to investigate the correlation between the *NOD2* genotype and its functional abnormality and the Blau syndrome/EOS clinical phenotype. Our findings suggest that *NOD2* genotyping may help predict disease progression in patients with Blau syndrome/EOS, although the clinical severity of Blau syndrome/EOS was not clearly associated with basal NF-κB activity due to mutated *NOD2* among the limited number of patients we studied.

The classic Blau syndrome/EOS symptom triad is skin rash, arthritis, and uveitis. Corresponding clinical manifestations include widespread erythematous papules, polyarthritis with boggy synovial swellings, and panuveitis (1,9,10,23), which were also identified in the present study. Rose et al described 2 patients who also had 1 episode of erythema nodosum–like lesions during the course of the disease (9). In our cohort, 5 patients had erythema nodosum–like lesions, suggesting that this should be recognized as one of the skin manifestations associated with Blau syndrome/EOS.

In the current study, 55% of the patients had fever, which always accompanied at least 1 symptom of the classic triad. Arostegui et al also reported that 50% of their cohort had recurrent or persistent fever (10). These findings suggest that fever is one of the important symptoms of Blau syndrome/EOS and is the reason why Blau syndrome/EOS is misdiagnosed as systemic-onset juvenile idiopathic arthritis (JIA). In fact, patient 11 in our study (who had the R334W mutation) experienced persistent fever reaching 40°C and received aggressive immunosuppressive therapy, because systemic-onset JIA was initially diagnosed. This case alerts us to the possibility that patients with Blau syndrome/EOS can sometimes have fever, and that Blau syndrome/EOS can resemble systemic-onset JIA.

Bilateral hilar lymph nodes, which are often seen in adult sarcoidosis, are not observed in Blau syndrome/EOS, but this does not mean that pulmonary lesions do not occur in patients with Blau syndrome/EOS. In fact, 2 patients (patient 5 [with the R334Q mutation] and patient 10 [with the R334W mutation]) had pulmonary lesions; in particular, patient 10 had the first reported case of sporadic EOS in association with the *NOD2* mutation (6). Another case of Blau syndrome/EOS with pulmonary lesions and interstitial pneumonitis, but not bilateral hilar lymph nodes, has also been reported (28). These findings suggest the importance of following up patients with Blau syndrome/EOS to check for not only the classic triad of symptoms but also other abnormalities, including pulmonary lesions.

Blau syndrome/EOS, which usually occurs in children younger than age 4 years, developed at 5 years and 8 years, respectively, in 2 patients in the present study (patient 2 [with the E383G mutation] and patient 17 [with the R334W mutation]). Because both of these patients had a family history of skin rash/arthritis/uveitis, they had been closely monitored by their parents as well as by their physicians. Therefore, it is unlikely that any symptoms that occurred when the patients were younger than 4 years of age were overlooked in these 2 cases. In the literature, there is 1 case of Blau syndrome in which skin rash, persistent fever, and camptodactyly started to develop at age 18 years (10). These findings indicate that the onset of Blau syndrome/EOS can be at age 5 years or older, and that disease onset in a patient younger than 4 years should not be considered requisite for a diagnosis of Blau syndrome/EOS.

In our cohort, the age at disease/symptom onset, organ involvement, and severity of Blau syndrome/EOS varied substantially even within affected families and between individuals with the same *NOD2* mutation (e.g., R334W). In other genetic disorders, identical mutations have been associated with phenotypic variation in unrelated individuals, within a family, and even in monozygotic twins (29). Phenotypic variation in Blau syndrome/EOS has been reported in monozygotic twins; therefore, nongenetic factors such as environmental conditions and/or infectious agents might be involved in phenotypic variation (24). Interestingly, in 2 of our cases, BCG vaccination was an obvious triggering factor. In addition, a previous report noted that cutaneous lesions first arose after BCG vaccination in a patient with Blau syndrome/EOS (30). The BCG vaccine contains muramyldipeptide, a ligand for NOD-2 protein (11,12), which is interesting from a pathophysiologic point of view. However, BCG vaccination did not always cause the onset of disease in patients with Blau syndrome/EOS, because most patients in our cohort were vaccinated with BCG according to the immunization protocol used in areas of

Japan where the risk for tuberculosis was high. An unknown endogenous ligand for NOD-2 could influence disease onset and/or progression, similar to uric acid as an endogenous cryopyrin/NLRP3 ligand (31). The potential roles of endogenous ligands, pathogen-associated molecular patterns, and/or danger-associated molecular patterns in disease pathogenesis remain to be elucidated.

Although increased basal NF-κB activity due to mutated *NOD2* has been proposed as an etiology of Blau syndrome/EOS, how such activity causes the characteristic symptoms remains unclear. We hypothesized that if increased basal NF-κB activity is the key to the pathophysiology of this disease, it should be related to disease severity or disease progression. Unfortunately, there was no clear correlation between basal NF-κB activity and the onset of disease/symptoms. However, patients with mutated *NOD2* and low basal NF-κB activity tended to experience complications, e.g., arthritis and uveitis, at a later age. This finding raises the possibility that basal NF-κB activity may affect disease progression rather than disease onset. Given that NOD-2 protein signals through MAPK/ERK as well as the NF-κB pathway (32), the possibility cannot be excluded that the MAPK/ERK activation potential of each *NOD2* genotype might also be correlated with disease severity or progression.

From the perspective of quality of life, the ocular manifestations of Blau syndrome/EOS require the closest attention (33). In a previous study, one-third of patients with Blau syndrome/EOS and *NOD2* mutations had a poor or extremely poor visual outcome, and the progression of visual field loss was independent of the particular *NOD2* mutant and was not associated with disease duration (9). In our cohort, however, patients with the R334W mutation experienced more visual impairment than did patients with the R334Q mutation, although 4 patients with the R334W mutation were from 2 families (patients 14 and 15 and patients 16 and 17, respectively). Therefore, familial genetic and environmental factors could easily influence the phenotype. Thus, in order not to favor our hypothesis, we excluded patients 15 and 17 from the analysis, and the trend was still evident. This observation was consistent with the findings of Rose et al (9), although those investigators did not address this issue. These findings suggest that *NOD2* genotyping could help predict the course of eye disease in patients with Blau syndrome/EOS, especially those with the R334Q mutation or the R334W mutation.

The relationship between visual impairment and basal NF-κB activity also remains a matter for discussion. Our data showed that visual impairments were more severe in patients with the R334W mutation than in those with the R334Q mutation, which seems to be consistent with the hypothesis that higher basal NF-κB activity causes more severe disease or more disease progression. However, no ocular symptoms have developed during the 6 years since disease onset in patient 20 (with the C495Y mutation and the highest basal NF-κB activity in our cohort), although ocular symptoms developed in another patient with the same genotype (10). Also, in patient 2, who had the E383G mutation and the lowest basal NF-κB activity, severe visual impairment occurred when she was in her late twenties. These findings contradict our hypothesis that *NOD2* genotypes with higher basal NF-κB activity are associated with severe disease. However, Blau syndrome/EOS was promptly diagnosed in patient 20 with the C495Y mutation, who luckily was under the care of the same pediatric rheumatologist who treated patient 19 (who had the N670K mutation) and was treated with systemic steroid therapy. Patient 2 (who had the E383G mutation) subsequently received inappropriate immunosuppressive therapy, because the patient refused steroid treatment. Furthermore, patient 10 (with the R334W mutation), who had no obvious systemic inflammatory findings and did not receive systemic steroid therapy, became blind at 20 years of age. These findings raise the possibility that the extent of visual impairment could be modified by therapy.

Finally, we were not able to prove a link between the clinical severity of Blau syndrome/EOS and basal NF-κB activity in the whole cohort, possibly because of the restricted number of patients and because of the differences in treatment among patients. Therefore, a prospective study involving a sufficient number of patients to allow analysis of each genotype–phenotype correlation would be required to test our hypothesis. Given that there is no standard treatment protocol for Blau syndrome/EOS, some predictors of disease progression, especially progression of visual impairment, would have great benefit for clinicians. We observed a difference in the development of visual impairment only between patients with the R334W mutation and those with the R334Q mutation, which provides a clue that predicts the development of visual impairment in patients with the R334W and R334Q mutations. We also believe that understanding the mechanisms of how *NOD2* acts in disease pathogenesis should help in discovering therapeutic targets for the treatment of Blau syndrome/EOS.

ACKNOWLEDGMENTS

We appreciate the invaluable assistance of the following physicians, who kindly provided materials and allowed us to study their patients: Drs. Sonoko Nagai, Takenosuke Yuasa, Akira Manki, Yoshihiko Sakurai, Mitsuru Nakajima, Hiroko Kobayashi, Ikuma Fujiwara, Hiroyuki Tsutsumi, Shuji Takei, Kumiko Nakao, Yoshikazu Otsubo, Kouichi Ohta, Kazunaga Agematsu, Hiroaki Azukisawa, Hiroyuki Murota, and Kenji Katamura.

AUTHOR CONTRIBUTIONS

Dr. Nishikomori had full access to all of the data in the study and takes responsibility for the integrity of the data and the accuracy of the data analysis.

Study design. Okafuji, Nishikomori, Heike, Miyachi, Nakahata.
Acquisition of data. Okafuji, Fujisawa, Saito, Yoshioka, Kawai, Sakai, Tanizaki.
Analysis and interpretation of data. Okafuji, Nishikomori.
Manuscript preparation. Okafuji, Nishikomori, Kanazawa, Kambe.
Statistical analysis. Yamazaki.

REFERENCES

1. Hetherington S. Sarcoidosis in young children. Am J Dis Child 1982;136:13–5.
2. Blau EB. Familial granulomatous arthritis, iritis, and rash. J Pediatr 1985;107:689–93.
3. Jabs DA, Houk JL, Bias WB, Arnett FC. Familial granulomatous synovitis, uveitis, and cranial neuropathies. Am J Med 1985;78:801–4.
4. Ohmen JD, Yang HY, Yamamoto KK, Zhao HY, Ma Y, Bentley LG, et al. Susceptibility locus for inflammatory bowel disease on chromosome 16 has a role in Crohn's disease, but not in ulcerative colitis. Hum Mol Genet 1996;5:1679–83.
5. Miceli-Richard C, Lesage S, Rybojad M, Prieur AM, Manouvrier-Hanu S, Hafner R, et al. CARD15 mutations in Blau syndrome. Nat Genet 2001;29:19–20.
6. Kanazawa N, Matsushima S, Kambe N, Tachibana T, Nagai S, Miyachi Y. Presence of a sporadic case of systemic granulomatosis syndrome with a CARD15 mutation. J Invest Dermatol 2004;122: 851–2.
7. Kanazawa N, Okafuji I, Kambe N, Nishikomori R, Nakata-Hizume M, Nagai S, et al. Early-onset sarcoidosis and CARD15 mutations with constitutive nuclear factor-κB activation: common genetic etiology with Blau syndrome. Blood 2005;105:1195–7.
8. Rose CD, Doyle TM, McIlvain-Simpson G, Coffman JE, Rosenbaum JT, Davey MP, et al. Blau syndrome mutation of CARD15/NOD2 in sporadic early onset granulomatous arthritis. J Rheumatol 2005;32:373–5.
9. Rose CD, Wouters CH, Meiorin S, Doyle TM, Davey MP, Rosenbaum JT, et al. Pediatric granulomatous arthritis: an international registry. Arthritis Rheum 2006;54:3337–44.
10. Arostegui JI, Arnal C, Merino R, Modesto C, Carballo MA, Moreno P, et al. NOD2 gene–associated pediatric granulomatous arthritis: clinical diversity, novel and recurrent mutations, and evidence of clinical improvement with interleukin-1 blockade in a Spanish cohort. Arthritis Rheum 2007;56:3805–13.
11. Girardin SE, Boneca IG, Viala J, Chamaillard M, Labigne A, Thomas G, et al. Nod2 is a general sensor of peptidoglycan through muramyl dipeptide (MDP) detection. J Biol Chem 2003; 278:8869–72.
12. Inohara N, Ogura Y, Fontalba A, Gutierrez O, Pons F, Crespo J, et al. Host recognition of bacterial muramyl dipeptide mediated through NOD2: implications for Crohn's disease. J Biol Chem 2003;278:5509–12.
13. Ogura Y, Inohara N, Benito A, Chen FF, Yamaoka S, Nunez G. Nod2, a Nod1/Apaf-1 family member that is restricted to monocytes and activates NF-κB. J Biol Chem 2001;276:4812–8.
14. Hugot JP, Chamaillard M, Zouali H, Lesage S, Cezard JP, Belaiche J, et al. Association of NOD2 leucine-rich repeat variants with susceptibility to Crohn's disease. Nature 2001;411:599–603.
15. Ogura Y, Bonen DK, Inohara N, Nicolae DL, Chen FF, Ramos R, et al. A frameshift mutation in NOD2 associated with susceptibility to Crohn's disease. Nature 2001;411:603–6.
16. Chamaillard M, Philpott D, Girardin SE, Zouali H, Lesage S, Chareyre F, et al. Gene-environment interaction modulated by allelic heterogeneity in inflammatory diseases. Proc Natl Acad Sci U S A 2003;100:3455–60.
17. Yotsumoto S, Takahashi Y, Takei S, Shimada S, Miyata K, Kanzaki T. Early onset sarcoidosis masquerading as juvenile rheumatoid arthritis. J Am Acad Dermatol 2000;43(5 Pt 2):969–71.
18. Ukae S, Tsutsumi H, Adachi N, Takahashi H, Kato F, Chiba S. Preschool sarcoidosis manifesting as juvenile rheumatoid arthritis: a case report and a review of the literature of Japanese cases. Acta Paediatr Jpn 1994;36:515–8.
19. Sakurai Y, Nakajima M, Kamisue S, Nishimura Y, Ueda T, Miyagawa S, et al. Preschool sarcoidosis mimicking juvenile rheumatoid arthritis: the significance of gallium scintigraphy and skin biopsy in the differential diagnosis. Acta Paediatr Jpn 1997;39:74–8.
20. Kurokawa T, Kikuchi T, Ohta K, Imai H, Yoshimura N. Ocular manifestations in Blau syndrome associated with a CARD15/Nod2 mutation. Ophthalmology 2003;110:2040–4.
21. Resnikoff S, Pascolini D, Etya'ale D, Kocur I, Pararajasegaram R, Pokharel GP, et al. Global data on visual impairment in the year 2002. Bull World Health Organ 2004;82:844–51.
22. North AF Jr, Fink CW, Gibson WM, Levinson JE, Schuchter SL, Howard WK, et al. Sarcoid arthritis in children. Am J Med 1970;48:449–55.
23. Lindsley CB, Petty RE. Overview and report on international registry of sarcoid arthritis in childhood. Curr Rheumatol Rep 2000;2:343–8.
24. Milman N, Andersen CB, Hansen A, van Overeem Hansen T, Nielsen FC, Fledelius H, et al. Favourable effect of TNF-α inhibitor (infliximab) on Blau syndrome in monozygotic twins with a de novo CARD15 mutation. APMIS 2006;114:912–9.
25. Rotenstein D, Gibbas DL, Majmudar B, Chastain EA. Familial granulomatous arteritis with polyarthritis of juvenile onset. N Engl J Med 1982;306:86–90.
26. Gross KR, Malleson PN, Culham G, Lirenman DS, McCormick AQ, Petty RE. Vasculopathy with renal artery stenosis in a child with sarcoidosis. J Pediatr 1986;108:724–6.
27. Rose CD, Eichenfield AH, Goldsmith DP, Athreya BH. Early onset sarcoidosis with aortitis: "juvenile systemic granulomatosis?" [published erratum appears in J Rheumatol 1990;17:575]. J Rheumatol 1990;17:102–6.
28. Becker ML, Martin TM, Doyle TM, Rose CD. Interstitial pneumonitis in Blau syndrome with documented mutation in CARD15. Arthritis Rheum 2007;56:1292–4.
29. Wolf U. Identical mutations and phenotypic variation [review]. Hum Genet 1997;100:305–21.
30. Osborne GE, Mallon E, Mayou SC. Juvenile sarcoidosis after BCG vaccination. J Am Acad Dermatol 2003;48(5 Suppl):S99–102.
31. Martinon F, Petrilli V, Mayor A, Tardivel A, Tschopp J. Gout-associated uric acid crystals activate the NALP3 inflammasome. Nature 2006;440:237–41.
32. Pauleau AL, Murray PJ. Role of Nod2 in the response of macrophages to Toll-like receptor agonists. Mol Cell Biol 2003; 23:7531–9.
33. Fink CW, Cimaz R. Early onset sarcoidosis: not a benign disease. J Rheumatol 1997;24:174–7.

European Journal of Haematology ISSN 0902-4441

ORIGINAL ARTICLE

AKR-501 (YM477) a novel orally-active thrombopoietin receptor agonist

Mari Fukushima-Shintani[1*], Ken-ichi Suzuki[2*], Yoshiyuki Iwatsuki[2], Masaki Abe[2], Keizo Sugasawa[2], Fukushi Hirayama[2], Tomihisa Kawasaki[3], Tatsutoshi Nakahata[4]

[1]QA, RA and Pharmacovigilance, Astellas Pharma Inc., Itabashi-ku, Tokyo, Japan; [2]Drug Discovery Research, Astellas Pharma Inc., Tsukuba, Ibaraki, Japan; [3]Development, Astellas Pharma Inc., Itabashi-ku, Tokyo, Japan; [4]Department of Pediatrics, Kyoto University Graduate School of Medicine, Shogoin, Sakyo-ku, Kyoto, Japan

Abstract

Thrombopoietin (TPO) is the principal physiologic regulator of platelet production. We have searched for small molecule compounds that mimic the action of TPO by using human TPO receptor-expressed in Ba/F3 cells, resulting in the discovery of AKR-501 (YM477). AKR-501 specifically targeted the TPO receptor and stimulated megakaryocytopoiesis throughout the development and maturation of megakaryocytes just as rhTPO did. AKR-501, however, was shown to be effective only in humans and chimpanzees with high species specificity. Therefore, we examined the *in vivo* platelet-increasing effect of AKR-501 in human platelet producing non-obese diabetic/severe combined immunodeficiency (NOD/SCID) mice transplanted with human fetal liver $CD34^+$ cells. Daily oral administration of AKR-501 dose-dependently increased the number of human platelets in these mice, with significance achieved at doses of 1 mg/kg and above. The peak unbound plasma concentrations of AKR-501 after administration at 1 mg/kg in NOD/SCID mice were similar to those observed following administration of an active oral dose in human subjects. These results suggest that AKR-501 is an orally-active TPO receptor agonist that may be useful in the treatment of patients with thrombocytopenia.

Key words thrombopoietin; thrombopoiesis; c-mpl; platelets; NOD/SCID mice; AKR-501; YM477

Correspondence Ken-ichi Suzuki, PhD., Pharmacology Research Laboratories, Astellas Pharma Inc., 21 Miyukigaoka, Tsukuba, Ibaraki 305-8585, Japan. Tel: +81 29 852 5111; Fax: +81 29 852 2955; e-mail: kenichi-suzuki@jp.astellas.com

*Contributed equally to this work.

Accepted for publication 26 November 2008

doi:10.1111/j.1600-0609.2008.01198.x

While platelet development appears to be regulated by a number of growth factors and cytokines, thrombopoietin (TPO) is the principal physiologic regulator of platelet production (1, 2). TPO stimulates megakaryocytopoiesis throughout the development and maturation of megakaryocytes leading to platelet production. The TPO receptor is expressed on hematopoietic stem cells (HSCs), a subfraction of hematopoietic precursors, and on cells of the megakaryocytic lineage and platelets. Two TPO receptor agonists, recombinant human TPO (rhTPO) and pegylated recombinant megakaryocyte growth and development factor (PEG-rHuMGDF), have previously undergone extensive clinical trials. However, the clinical development of PEG-rHuMGDF was terminated because of the development of neutralizing antibodies to PEG-rHuMGDF that cross-reacted with endogenous thrombopoietin, resulting in profound hematological consequences in patients and volunteers receiving multiple subcutaneous injections of the drug (3, 4). The appearance of antibodies was reported in an early trial of rhTPO, but the biological activity of these antibodies has not been reported (5). Recombinant

TPOs are therefore associated with risk of immunogenicity.

Recently, a number of screening methods have been developed to identify small molecules that could mimic the biological effects of hematopoietic growth factors. Potential advantages of small molecule mimetics include their putative lack of immunogenicity and non-parenteral route of administration. Small molecules might also be less expensive to produce. To identify small molecule mimetics of native proteins, high throughput assays of either receptor binding or biological activity have been devised. With respect to TPO, several small molecular compounds were reported to mimic the effect of TPO through the TPO receptor (6–10). Therefore, we screened by using human TPO receptor transfected murine Ba/F3 cells to identify orally active small molecular TPO receptor agonists (11), which led to the discovery of AKR-501.

Here, we describe the pharmacological properties of AKR-501. We showed that AKR-501 mimics the biological activities of TPO *in vitro* and *in vivo*. AKR-501, however, was showed to have effect in humans and chimpanzees only. Non-obese diabetic/severe combined immunodeficiency (NOD/SCID) mice were characterized as representing an efficient engraftment model for human HSCs, which resulted in the production of human platelets. Therefore, this model was used in this study to examine the effect of AKR-501 on *in vivo* platelet production in human platelet producing NOD/SCID mice in which human HSCs has been transplanted. Further, we demonstrated that this model is suitable to predict the effect of AKR-501 in humans.

Materials and methods

Compounds

AKR-501, 1-(3-Chloro-5-{[4-(4-chloro-2-thienyl)-5-(4-cyclohexylpiperazin-1-yl)-1,3-thiazol-2-yl]carbamoyl}-2-pyridyl) piperidine-4-carboxylic acid was synthesized by Yamanouchi Pharmaceutical Co., Ltd. (Ibaraki, Japan) (12). rhTPO was purchased from GT (Minneapolis, MN, USA).

Human TPO receptor expressed Ba/F3 cells

The human full-length *c-mpl* cDNA (*c-mpl-p*) derived from HEL cells was subcloned into a pEF-BOS vector. This plasmid pEF-BOS-*c-mpl* (10 μg) and the selection marker plasmid pSV2bsr (1 μg) (Kaken-Seiyaku, Tokyo, Japan) were co-electroporated into murine IL-3 (mIL-3) dependent murine Ba/F3 cells in a 0.4 cm cuvette at 1.5 kV (25 μF). These cells were then cultured in RPMI 1640 medium (GIBCO, Grand Island, NY, USA) supplemented with WEHI conditioned media (BD Biosciences, Bedford, MA, USA) for 3 d, and then in selection medium containing 10 μg/mL blasticidin (Funakoshi, Tokyo, Japan) for 1 month.

Assay for TPO receptor-dependent cell growth

The cells used in this study were maintained in RPMI 1640 medium supplemented with 10% FBS (JRH BIOSCIENCES, Lenexa, KS, USA), 50 units/mL penicillin/streptomycin (GIBCO), and WEHI conditioned media. These cells were seeded in each well of a 96-well plate and cultured in the medium at the concentration of 2×10^5 cells/mL. Human TPO receptor expressing Ba/F3 cells were incubated with AKR-501, dissolved in dimethyl sulfoxide (DMSO), or rhTPO. Ba/F3 cells were incubated with AKR-501, rhTPO or recombinant mIL-3 (rmIL-3; Pepro Tech EC, London, UK). WST-1/1-methoxy PMS reagent (Cell counting kit, Dojin, Kumamoto, Japan) was added to each well and then incubated. A450/A655 was measured with a microplate reader (Model 3350; BioRad, Hercules, CA, USA) immediately and at 2 h after addition of WST-1/1-methoxy PMS reagent. Proliferation activity of the compound was calculated as the percentage of maximum proliferative activity of rhTPO for TPO receptor expressing Ba/F3 cells. The percentage of maximum proliferative activity of rmIL-3 was used to calculate the proliferation activity for Ba/F3 cells.

Megakaryocyte colony formation

Human cord blood (CB) $CD34^+$ cells (AllCells, Berkeley, CA, USA) at a density of 2500 cells/0.75 mL were suspended in MegaCult™-C (StemCell Technologies Inc., Vancouver, Canada) containing either AKR-501 dissolved in DMSO or rhTPO, and plated in two-well chamber slides. After 10–12 d of incubation, human CD41-positive megakaryocytes were identified. Colonies that contained three or more human CD41-positive cells were scored as human megakaryocyte colonies. Data were expressed as the percentage of maximum differentiation activity of rhTPO, and the EC_{50} values were calculated for the drug.

Ploidy analysis

G-CSF-mobilized human peripheral blood $CD34^+$ cells (BioWhittaker Inc., Walkersville, MD, USA) were seeded in a 24-well culture plate (Iwaki, Chiba, Japan) at 10 000 cells/0.5 mL/well in culture medium in the presence of 3 μM AKR-501 or 3 nM rhTPO. The culture medium consisted of 100 μM 2-mercaptoethanol, 7.5 μg/mL

cholesterol, BIT9500 (StemCell Technologies Inc.), and Iscove's modified Dulbecco's medium. The cells were cultured for 12 d at 37°C. The cells were collected and stained with anti-human CD41-FITC (BD PharMingen, San Diego, CA, USA). After incubation for 20 min at 4°C, cells were washed, made permeable by gradual addition of methanol which was chilled at −40°C, and incubated for 30 min at 4°C. Then, cells were treated with 100 μg/mL RNase (Nippon Gene, Toyama, Japan) for 30 min at 4°C, and 50 μg/mL propidium iodide (PI) (Sigma, St. Louis, MO, USA) was added. After incubation for 30 min under darkness at 4°C, the cells were suspended in 500 μL of 2% FBS-PBS and analyzed using a flow cytometry (EPICS XL-MCL, Beckman-Coulter, Miami, FL, USA). Cells expressing CD41 were regarded as megakaryocytes. Ploidy distribution was analyzed by histogram. Events of each peak were counted by setting markers. Each ploidy level was expressed as event %. Event % at ploidy level of nN was calculated by the followed equation; Events % (nN) = [nN/(2N + 4N + 8N + 16N + 32N<)] × 100.

Western blot analysis of signal transduction through TPO receptor

Human TPO receptor expressing Ba/F3 cells washed free of growth factors by media, were incubated in RPMI1640 supplemented with 10% FBS and 50 units/mL penicillin/streptomycin for 15 h at 37°C. After this depletion period, cells were resuspended in RPMI1640 at a concentration of 1×10^6/mL and were stimulated with either AKR-501 or rhTPO at 37°C for 15 min. Cells were lysed in the same volume of a buffer containing 15 mM HEPES (pH 7.4), 150 mM NaCl, 10 mM EGTA, 1 mM sodium orthovanadate, protease inhibitor cocktail tablet (Roche Diagnostics, Indianapolis, IN, USA), and 2% (w/v) Triton X-100. Insoluble materials were removed by centrifugation at 10 000 × *g* for 30 min at 4°C. Total lysates were separated by electrophoresis using an SDS-PAGE gel under reducing conditions and transferred to a sheet of polyvinylidene difluoride membrane (Millipore, Bedford, MA, USA). The membrane was then blocked with Block Ace (Dainihon-Seiyaku, Osaka, Japan) at room temperature for 30 min. Membranes were then incubated overnight at 4°C in a hybridization buffer consisting of anti-phospho-STAT3 (Tyr705), anti-phospho-STAT5 (Tyr694), and anti-phospho-ERK (Thr202, 204) antibodies (Cell Signaling, Beverly, MA, USA) in Tris-buffered saline with 0.05% Tween 20 (TBST), and 3% FBS. These filters were stripped and reprobed with anti-STAT3, anti-STAT5 (Santa Cruz Biotechnology, CA, USA), and anti-ERK antibodies (Upstate Biotechnology, Lake Placid, NY, USA) to assure equal loading in each lane of the gel. Blots were developed using an ECL kit (Amersham Pharmacia, Buckinghamshire, UK).

Western blot analysis of tyrosine phosphorylation of STAT 5 in the platelets

Human blood was drawn from healthy volunteers in the presence of a 1/10th volume of 3.8% sodium citrate, added as an anticoagulant, and centrifuged at 150 × *g* for 10 min to obtain platelet-rich plasma (PRP). Animal blood from various species (chimpanzee, olive baboon, rhesus monkey, cynomolgus monkey, common marmoset, squirrel monkey, beagle dog, guinea pig, rabbit, rat, and hamster) were drawn in the presence of 1/10th volume of 3.8% sodium citrate. PRP was prepared by centrifugation of whole blood at 170 × *g* for 10 min. After the addition of 5 nM PGE_1 (Sigma), 5 mM EDTA (pH 8.05), and 3 U/mL apyrase (Sigma), the PRP was centrifuged at 1490 × *g* to form a platelet pellet. The pellet was resuspended in 5 mL of a Tyrode's-HEPES buffer (137 mM NaCl, 2.68 mM KCl, 3.75 mM NaH_2PO_4, 0.98 mM $MgCl_2$, 5.55 mM dextrose, 0.35% (w/v) BSA, and 37.8 mM HEPES, pH 6.7) also containing 5 nM PGE_1, 5 mM EDTA (pH 8.05), and 3 U/mL apyrase and washed once. For western blot analysis, platelets were resuspended at a concentration of 3×10^8 cells/mL in the Tyrode's-HEPES buffer (pH 7.35) and were stimulated with either AKR-501 or rhTPO at 37°C for 15 min. The Western blot protocol was as described above. In the incubation process, membranes were in a hybridization buffer consisting of anti-phospho-STAT5 antibody in TBST and 3% FBS.

Transplantation of human fetal liver $CD34^+$ cells into NOD/SCID mice

Human fetal liver (FL) $CD34^+$ cells (approximately 1 00 000 cells/mouse, BioWhittaker Inc, Walkersville, MD, USA) were injected into 9- to 12-wk-old NOD/SCID mice through the tail vein after irradiation with 2.4 Gy as two divided doses at intervals of at least 4 h by an X-ray apparatus (MBR-1520R-3, Hitachi Medical Corporation, Tokyo, Japan). The transplanted mice were injected intraperitoneally with anti-asialo GM1 antiserum (Wako, Osaka, Japan) immediately before cell transplantation and every 9–11 d after cell transplantation, a total of six times in order to deplete natural killer cells. After transplantation, mice were given sterile water containing prophylactic neomycin. Peripheral blood (PB) was obtained from the retro-orbital plexus using heparinized calibrated pipets (Drummond Scientific Co, Broomall, PA, USA), and transferred to EDTA 2Na containing Capiject (Terumo Medical, Somerset, NJ, USA). Blood cell counts were measured

using an automatic cell counter (MEK-6258, Nihon Kohden, Tokyo, Japan).

Flow cytometric analysis of peripheral blood in transplanted NOD/SCID mice

Human platelets from NOD/SCID mice were analyzed by flow cytometry (EPICS XL-MCL). Human platelets in PB were measured by staining with anti-human CD41-PE and anti-murine CD41-FITC (BD PharMingen). The percentage of human platelets was calculated by dividing the number of $hCD41^+$ cells by the total number of $CD41^+$ cells (human and mouse). The number of human platelets in PB was calculated by multiplying the percentage of human platelets by the total blood platelet count in PB, as measured with an automatic cell counter. The number of murine platelets in PB was calculated by subtracting the number of human platelets from the total platelet count.

Administration of AKR-501 to transplanted NOD/SCID mice

Various doses of AKR-501 (0, 0.3, 1, and 3 mg/kg/d), suspended in 0.5% methylcellulose, were orally administered for 14 d to NOD/SCID mice transplanted with human FL $CD34^+$ cells. PB was collected on days 7, 14, 21, and 28 after the start of AKR-501 administration, and blood cell counts and the number of human platelets were measured. The time course of changes in human and murine platelets number is expressed in terms of the rate of increase after administration of AKR-501 relative to the value at predosing. Statistical analysis was performed by Dunnett's test.

Results

AKR-501 is a TPO receptor agonist

We screened for small molecule compounds that mimic the action of TPO using a method that measured the proliferative activity of human TPO receptor-expressing Ba/F3 cells, resulting in the discovery of an orally active TPO receptor agonist, AKR-501. AKR-501 supported the proliferation of TPO receptor expressing Ba/F3 cell in a concentration-dependent fashion (Fig. 1A). The compound demonstrated an EC_{50} value of 3.3 ± 0.2 nM in this assay with the maximum proliferative activity equivalent to maximum activity of rhTPO. The activity of the compound was dependent on the TPO receptor, because parental Ba/F3 cells did not respond to either AKR-501 or rhTPO (Fig. 1A, B). Further, AKR-501 induced tyrosine phosphorylation of STAT3 and STAT5, and threonine phosphorylation of ERK in the cells, as

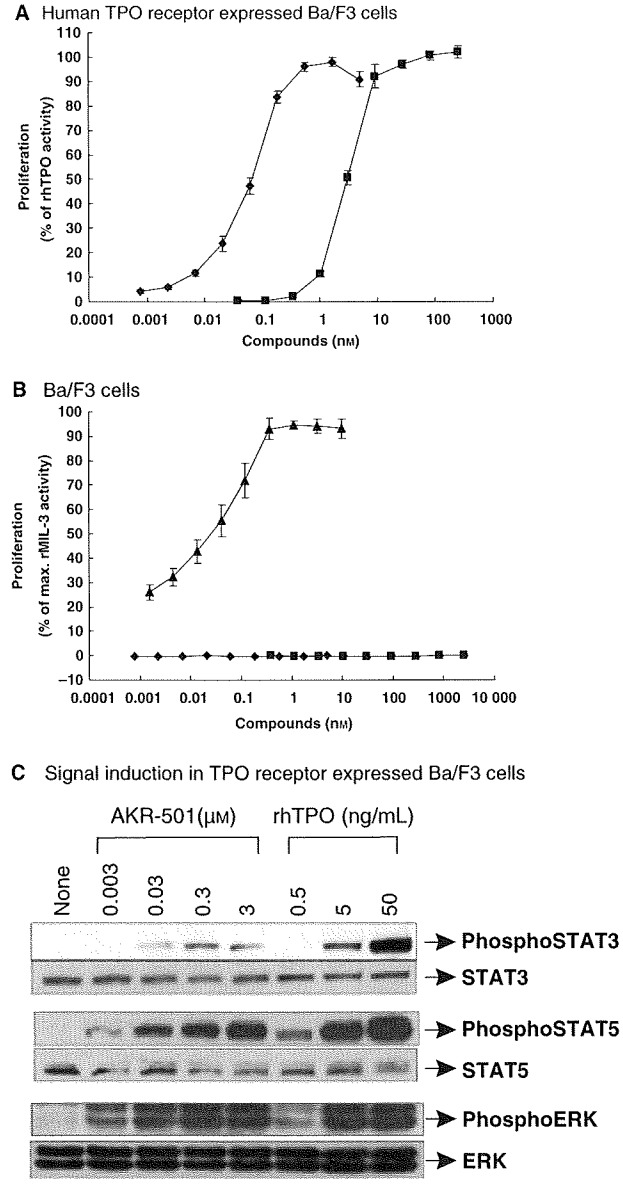

Figure 1 AKR-501 specifically acts on human Thrombopoietin (TPO) receptor. (A, B) Proliferative response of human TPO receptor expressed Ba/F3 cells (A) and Ba/F3 cells (B) to AKR-501 (■), rhTPO (♦), and rmIL-3 (▲). Data are presented as mean ± SE (n = 5). (C) Signal induction in TPO receptor expressed Ba/F3 cells. Human TPO receptor expressed Ba/F3 cells were stimulated by AKR-501 or rhTPO. Immunoblots were probed with anti-phospho-STAT3, anti-phospho-STAT5, and anti-phospho-ERK antibodies. These filters were stripped and reprobed with anti-STAT3, anti-STAT5, and anti-ERK antibodies.

did rhTPO. Thus, AKR-501 activates signal transduction in TPO receptor expressing Ba/F3 cells through the TPO receptor, and supports the proliferation of these cells (Fig. 1C).

TPO specifically stimulates megakaryocytopoiesis throughout the development and maturation of

megakaryocytes. Therefore, we examined the effect of AKR-501 on the differentiation to megakaryocytes from hematopoietic progenitor cells. AKR-501 promoted megakaryocyte colony formation from human CB $CD34^+$ cells in a concentration-dependent fashion (Fig. 2A). The EC_{50} value was 25.0 ± 7.8 nM for AKR-501 and the maximum activity of AKR-501 was similar to that of rhTPO. Human megakaryocyte colonies generated with AKR-501 and rhTPO had similar morphologic features (Fig. 2B, C). Further, AKR-501 and rhTPO induced polyploidization of megakaryocytes from G-CSF mobilized peripheral blood $CD34^+$ cells in liquid culture (Fig. 3A, B). There was no apparent difference between AKR-501 and rhTPO at each ploidy level (Fig. 3C). These results suggest that AKR-501 mimics the effect of TPO *in vitro*.

Species specificity of AKR-501

TPO receptor is expressed on the surface of platelets, and TPO induces signal transduction including STAT5. The species specificity of AKR-501 for the TPO receptor was demonstrated by STAT5 activation in platelets of various species (Fig. 4). AKR-501 induced tyrosine phosphorylation of STAT5 in human blood platelets and chimpanzee blood platelets, as did rhTPO. In contrast, rhTPO induced tyrosine phosphorylation of STAT5 in olive baboon, cynomolgus monkey, rhesus monkey, common marmoset, squirrel monkey, beagle dog, guinea pig, rabbit, rat, and hamster platelets (data not shown), but AKR-501 did not induce phosphorylation in these species.

Evaluation of AKR-501 on human platelet production in NOD/SCID mice

AKR-501 was shown to have strict species-specificity and to be effective only in humans and chimpanzees. To examine the *in vivo* pharmacological effects of AKR-501 on human platelet production, we used NOD/SCID mice transplanted with FL $CD34^+$ cells. NOD/SCID mice were characterized as an efficient engraftment model for HSCs. It had been reported that the multilineages of human hematopoiesis, including the production of human platelets, could be reconstituted over a long period of time in NOD/SCID mice transplanted with human HSCs (13, 14). In this study, we used commercially available cryopreserved human FL $CD34^+$ cells as a source of HSCs.

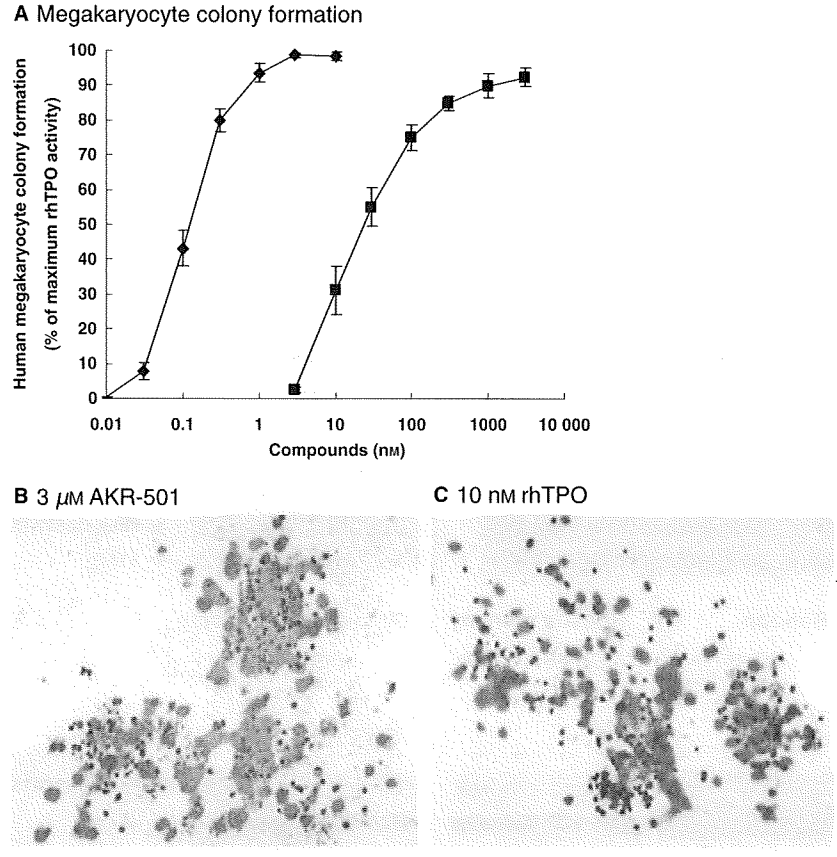

Figure 2 AKR-501 promotes megakaryocyte differentiation from human $CD34^+$ cells. (A) Megakaryocyte colony formation was measured in serum-free collagen-based medium cultures of human cord blood $CD34^+$ cells in the presence of increasing concentrations of AKR-501 (■), and recombinant human TPO (rhTPO) (♦). Data are presented as mean ± SE (n = 5). (B, C) Immunohistochemical identification of typical human megakaryocyte colonies generated with 3 μM AKR-501 (B) and 10 nM rhTPO (C) × 100 objectives.

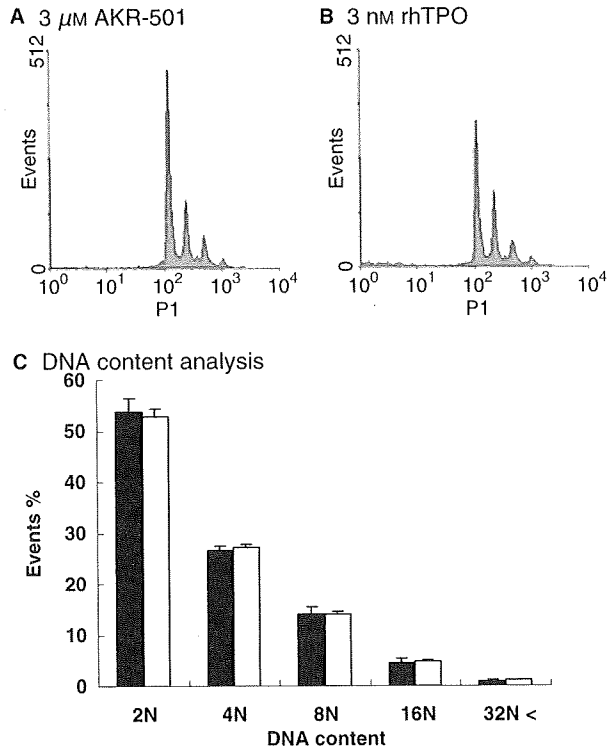

Figure 3 AKR-501 induces polyploidization of megakaryocytes. G-CSF-mobilized human peripheral blood $CD34^+$ cells were cultured for 12 d in serum-free liquid medium in the presence of 3 μM AKR-501 or 3 nM recombinant human TPO (rhTPO). Following surface marker staining, DNA analysis was performed by staining with propidium iodide. The plots show the typical ploidy distribution after gating on $CD41^+$ cells (A: 3 μM AKR-501, B: 3 nM rhTPO). (C) Ploidy analysis of megakaryocytes generated by 3 μM AKR-501 (open columns) or 3 nM rhTPO (filled columns). The data represent the mean ± SE of five independent experiments. Statistical analysis was performed in each DNA content group using Student's *t*-test.

Human platelets started to appear in the PB of these mice 4 wk after transplantation. The production of human platelets continued for more than 6 months post-transplant.

Doses of 0.3, 1, and 3 mg/kg/d of AKR-501 were orally administered once per day for 14 d to NOD/SCID mice that stably produced human platelets. Oral administration of AKR-501 dose-dependently increased the number of human platelets, resulting in approximately a 2.7-fold increase at 1 mg/kg/d ($P < 0.05$) and a 3.0-fold increase ($P < 0.01$) at 3 mg/kg/d on day 14 after the start of administration (Fig. 5A). The minimum effective dose was 1 mg/kg/d. Withdrawal of AKR-501 administration caused the human platelet count to return nearly to pretreatment levels. As was expected given the species selective activity of AKR-501, the murine platelet count did not change after oral administration of AKR-501 at any dosage (Fig. 5B). Further, WBC, RBC, and body weight did not significantly change during the study period (data not shown).

Discussion

We successfully employed high throughput screening techniques based on proliferation of human TPO receptor-expressing Ba/F3 cells to identify a series of 2-acylaminothiazole derivatives as a potent novel series of TPO receptor agonists. The lead agent in the series, AKR-501, caused dose-dependent proliferation of human TPO receptor-expressing Ba/F3 cells and promoted differentiation to human megakaryocytes. This agent was efficacious following oral administration, producing a dose-dependent increase of human platelet numbers in NOD/SCID mice transplanted with human FL $CD34^+$ cells.

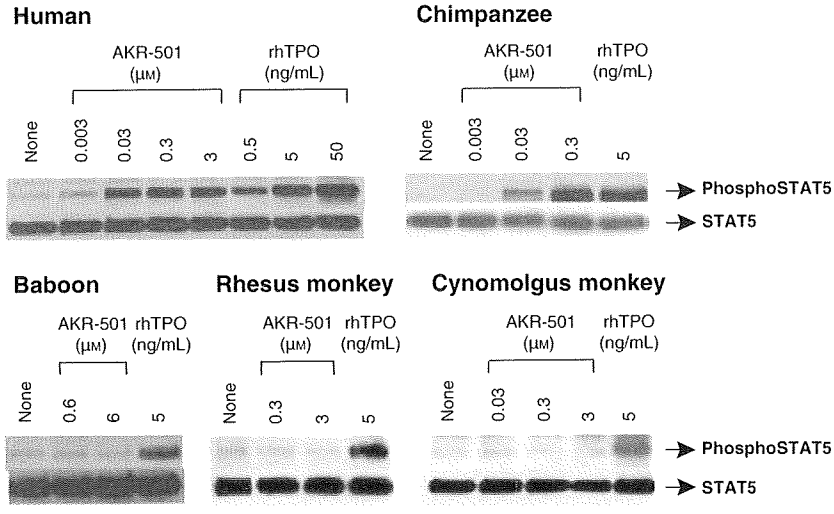

Figure 4 AKR-501 activates STAT5 in human and chimpanzee platelets, but not in baboon, rhesus, and cynomolgus monkey platelets. Human and non-human primate platelets were stimulated by AKR-501 or recombinant human TPO (rhTPO). Immunoblots were probed with anti-phospho-STAT5 antibody. These filters were stripped and reprobed with anti-STAT5 antibody.

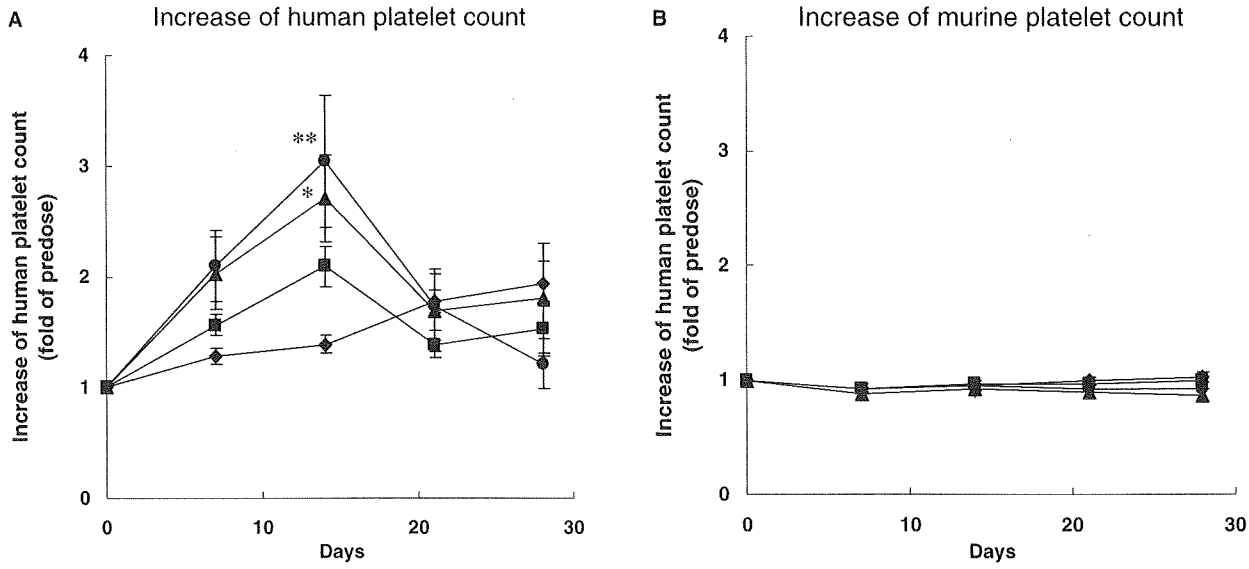

Figure 5 Oral administration of AKR-501 increases the number of human platelets in NOD/SCID mice transplanted with human FL CD34$^+$ cells. AKR-501 (vehicle (♦), 0.3 (■), 1 (▲), and 3 (•) mg/kg/d) was orally administered for 14 d to human platelet-producing NOD/SCID mice. PB was collected on the indicated days, and blood cell counts were measured. The percentage of human platelets was measured by flow cytometry, and the number of human (A) and murine platelets (B) was calculated as described in 'Materials and methods'. The time course of changes in human and murine platelet count is expressed in terms of the fold increase after administration of AKR-501 relative to the value at predosing. Data are presented as mean ± SE (n = 10, on day 28; n = 9 for vehicle, 0.3, 3 mg/kg/d groups). *$P < 0.05$, **$P < 0.01$ vs. vehicle group by Dunnett's test.

Other small molecules such as TM41 (15), SB-497115 (eltrombopag) (16), SB-394725 (17), and NIP-004 (18) have been reported as TPO receptor agonists. Some compounds including eltrombopag, SB-394725, and NIP-004 display species specificities (17–19) as did the compounds in our series. In order to identify an orally active TPO receptor agonist, we utilized NOD/SCID mice transplanted with human FL CD34$^+$ cells to evaluate hematopoietic stem cells (20–22) and human platelet production (13, 14). Previously we reported that subcutaneous injection of TPO to NOD/SCID mice transplanted with human cord blood CD34$^+$ cells dose-dependently increased the number of human platelets (14), and subcutaneous injection of NIP-004 has been shown to induce human platelet production in a xenotransplatation model (18). Herein we report that oral administration of AKR-501 to the NOD/SCID mice model increased the number of human platelets. To our knowledge, no other TPO agonists have been reported to be orally administered to the NOD/SCID mice model. Therefore, AKR-501 is the first TPO receptor agonist whose platelet increasing effect was proven by oral administration to NOD/SCID mice transplanted with human hematopoietic stem cells.

The efficacy of AKR-501 seen in the non-clinical model has also been demonstrated in the clinic. In a phase I study, once daily oral administration of AKR-501 at 10 mg to healthy volunteers for 14 d increased the number of platelets, resulting in a >50% increase over baseline platelet count (23). This result is consistent with the *in vivo* result using NOD/SCID mice transplanted with human FL CD34$^+$ cells. Furthermore, similar peak unbound plasma concentrations of AKR-501 were observed in both the non-clinical model and in this phase I clinical trial. The peak unbound plasma concentrations of AKR-501 after administration at 1 mg/kg in the NOD/SCID mice study and after 14 d dosing at 10 mg/d in human study were 3.3 and 3.4 ng/mL, respectively. The observed pharmacodynamic responses at comparable exposures demonstrate that the NOD/SCID model is suitable for predicting the concentration-effect relationship of orally-active TPO receptor agonists in man.

In conclusion, we identified a novel orally-active TPO receptor agonist, AKR-501, which mimics the biological activity of TPO both *in vitro* and *in vivo*. These non-clinical results and early results from clinical investigations suggest that AKR-501 is an orally active TPO receptor agonist that may prove useful for treating patients with thrombocytopenia.

Acknowledgements

We gratefully acknowledge Dr. Robert E. Desjardins for reviewing the manuscript and Dr. Stephen J. Waters for editing the manuscript.

Authorship

Contribution: M.F-S. performed research, analyzed data, and wrote the paper, K.Suzuki designed research, performed research, analyzed data and edited the paper, Y.I., M.A. and K.Sugasawa performed research, F.H. analyzed data, T.K. analyzed data and edited the paper, and T.N supervised the study.

Conflict-of-interest disclosure

Tatsutoshi Nakahata declares no competing financial interests. Other authors are employees of Astellas Pharma Inc.

References

1. Kaushansky K. Thrombopoietin. *N Engl J Med* 1998;**339**:746–54.
2. Kaushansky K, Drachman JG. The molecular and cellular biology of thrombopoietin: the primary regulator of platelet production. *Oncogene* 2002;**21**:3359–67.
3. Li J, Yang C, Xia Y, Bertino A, Glaspy J, Roberts M, Kuter DJ. Thrombocytopenia caused by the development of antibodies to thrombopoietin. *Blood* 2001;**98**:3241–8.
4. Basser RL, O'Flaherty E, Green M, Edmonds M, Nichol J, Menchaca DM, Cohen B, Begley CG. Development of pancytopenia with neutralizing antibodies to thrombopoietin after multicycle chemotherapy supported by megakaryocyte growth and development factor. *Blood* 2002;**99**:2599–602.
5. Vadhan-Raj S, Murray LJ, Bueso-Ramos C, *et al.* Stimulation of megakaryocyte and platelet production by a single dose of recombinant human thrombopoietin in patients with cancer. *Ann Intern Med* 1997;**126**:673–81.
6. Kuter DJ. New thrombopoietic growth factors. *Blood* 2007;**109**:4607–16.
7. Reiter LA, Subramanyam C, Mangual EJ, *et al.* Pyrimidine benzamide-based thrombopoietin receptor agonists. *Bioorg Med Chem Lett* 2007;**17**:5447–54.
8. Alper PB, Marsilje TH, Mutnick D, *et al.* Discovery and biological evaluation of benzo[a]carbazole-based small molecule agonists of the thrombopoietin (Tpo) receptor. *Bioorg Med Chem Lett* 2008;**18**: 5255–8.
9. Marsilje TH, Alper PB, Lu W, *et al.* Optimization of small molecule agonists of the thrombopoietin (Tpo) receptor derived from a benzo[a]carbazole hit scaffold. *Bioorg Med Chem Lett* 2008;**18**:5259–62.
10. Reiter LA, Jones CS, Brissette WH, *et al.* Molecular features crucial to the activity of pyrimidine benzamide-based thrombopoietin receptor agonists. *Bioorg Med Chem Lett* 2008;**18**:3000–6.
11. Duffy KJ, Darcy MG, Delorme E, *et al.* Hydrazinonaphthalene and azonaphthalene thrombopoietin mimics are nonpeptidyl promoters of megakaryocytopoiesis. *J Med Chem* 2001;**44**:3730–45.
12. Fukushima-Shintani M, Suzuki K, Iwatsuki Y, Abe M, Sugasawa K, Hirayama F, Kawasaki T. AKR-501 (YM477) in combination with thrombopoietin enhances human megakaryocytopoiesis. *Exp Hematol* 2008;**36**:1337–42.
13. Ueda T, Yoshino H, Kobayashi K, Kawahata M, Ebihara Y, Ito M, Asano S, Nakahata T, Tsuji K. Hematopoietic repopulating ability of cord blood CD34(+) cells in NOD/Shi-scid mice. *Stem Cells* 2000;**18**:204–13.
14. Suzuki K, Hiramatsu H, Fukushima-Shintani M, Heike T, Nakahata T. Efficient assay for evaluating human thrombopoiesis using NOD/SCID mice transplanted with cord blood $CD34^+$ cells. *Eur J Haematol* 2007;**78**:123–30.
15. Kimura T, Kaburaki H, Tsujino T, Ikeda Y, Kato H, Watanabe Y. A non-peptide compound which can mimic the effect of thrombopoietin via c-Mpl. *FEBS Lett* 1998;**428**:250–4.
16. Erickson-Miller C, Delorme E, Giampa L, *et al.* Biological Activity and Selectivity for Tpo Receptor of the Orally Bioavailable, Small Molecule Tpo Receptor Agonist, SB-497115. *Blood (ASH Annual Meeting Abstracts)* 2004;**104**:2912.
17. Erickson-Miller CL, DeLorme E, Tian SS, *et al.* Discovery and characterization of a selective, nonpeptidyl thrombopoietin receptor agonist. *Exp Hematol* 2005;**33**:85–93.
18. Nakamura T, Miyakawa Y, Miyamura A, Yamane A, Suzuki H, Ito M, Ohnishi Y, Ishiwata N, Ikeda Y, Tsuruzoe N. A novel nonpeptidyl human c-Mpl activator stimulates human megakaryopoiesis and thrombopoiesis. *Blood* 2006;**107**:4300–7.
19. Erickson-Miller CL, Delorme E, Iskander M, *et al.* Species Specificity and Receptor Domain Interaction of a Small Molecule TPO Receptor Agonist. *Blood (ASH Annual Meeting Abstracts)* 2004;**104**:2909.
20. Dick JE, Bhatia M, Gan O, Kapp U, Wang JC. Assay of human stem cells by repopulation of NOD/SCID mice. *Stem Cells* 1997;**15**:199–203.
21. Greiner DL, Hesselton RA, Shultz LD. SCID mouse models of human stem cell engraftment. *Stem Cells* 1998;**16**:166–77.
22. Dao MA, Nolta JA. Immunodeficient mice as models of human hematopoietic stem cell engraftment. *Curr Opin Immunol* 1999;**11**:532–7.
23. Desjardins RE, Tempel DL, Lucek R, Kuter DJ. Single and multiple oral doses of AKR-501 (YM477) increase the platelet count in healthy volunteers. *ASH Annual Meeting Abstracts* 2006;**108**:477.

THE JOURNAL OF BIOLOGICAL CHEMISTRY VOL. 284, NO. 13, pp. 8548–8556, March 27, 2009

FBP17 Mediates a Common Molecular Step in the Formation of Podosomes and Phagocytic Cups in Macrophages*[S]

Received for publication, July 23, 2008, and in revised form, December 29, 2008 Published, JBC Papers in Press, January 20, 2009, DOI 10.1074/jbc.M805638200

Shigeru Tsuboi[‡1], **Hidetoshi Takada**[§], **Toshiro Hara**[§], **Naoki Mochizuki**[¶], **Tomihisa Funyu**[‖], **Hisao Saitoh**[‖], **Yuriko Terayama**[‖], **Kanemitsu Yamaya**[‖], **Chikara Ohyama**[**], **Shigeaki Nonoyama**[‡‡], **and Hans D. Ochs**[§§]

From the [‡]Infectious and Inflammatory Disease Center, Burnham Institute for Medical Research, La Jolla, California 92037, the [§]Department of Pediatrics, Graduate School of Medical Sciences, Kyushu University, Fukuoka 812-8582, Japan, the [¶]Department of Structural Analysis, National Cardiovascular Center Research Institute, Osaka 565-8565, Japan, the [‖]Oyokyo Kidney Research Institute, Hirosaki 036-8243, Japan, the [**]Department of Urology, Hirosaki University School of Medicine, Hirosaki 036-8562, Japan, the [‡‡]Department of Pediatrics, National Defense Medical College, Saitama 359-0042, Japan, and the [§§]Department of Pediatrics, Research Center for Immunity and Immunotherapy, Seattle Children's Hospital Research Institute, Seattle, Washington 98101

Macrophages act to protect the body against inflammation and infection by engaging in chemotaxis and phagocytosis. In chemotaxis, macrophages use an actin-based membrane structure, the podosome, to migrate to inflamed tissues. In phagocytosis, macrophages form another type of actin-based membrane structure, the phagocytic cup, to ingest foreign materials such as bacteria. The formation of these membrane structures is severely affected in macrophages from patients with Wiskott-Aldrich syndrome (WAS), an X chromosome-linked immunodeficiency disorder. WAS patients lack WAS protein (WASP), suggesting that WASP is required for the formation of podosomes and phagocytic cups. Here we have demonstrated that formin-binding protein 17 (FBP17) recruits WASP, WASP-interacting protein (WIP), and dynamin-2 to the plasma membrane and that this recruitment is necessary for the formation of podosomes and phagocytic cups. The N-terminal EFC (extended FER-CIP4 homology)/F-BAR (FER-CIP4 homology and Bin-amphiphysin-Rvs) domain of FBP17 was previously shown to have membrane binding and deformation activities. Our results suggest that FBP17 facilitates membrane deformation and actin polymerization to occur simultaneously at the same membrane sites, which mediates a common molecular step in the formation of podosomes and phagocytic cups. These results provide a potential mechanism underlying the recurrent infections in WAS patients.

Podosomes (see Fig. 1*A*) are micron-scale, dynamic, actin-based protrusions observed in motile cells such as macrophages, dendritic cells, osteoclasts, certain transformed fibroblasts, and carcinoma cells (1). Podosomes play an important role in macrophage chemotactic migration, which is critical for recruitment of leukocytes to inflamed tissues. Podosomes are both adhesion structures and the sites of extracellular matrix degradation (2). Adhesion to and degradation of the extracellular matrix are essential processes for the successful migration of macrophages in tissues. Podosomes occur in most macrophages and can be observed by differentiating human primary monocytes into macrophages with macrophage-colony stimulating factor-1 (M-CSF-1)[2] and staining the F-actin using phalloidin (3, 4). Podosomes labeled in this way appear as F-actin-rich dots (see Fig. 1*C*). Podosome formation has recently been directly observed *in vitro* and *in vivo* in leukocyte migration through the endothelium, diapedesis (5).

Phagocytosis of bacterial pathogens is one of the most important primary host defense mechanisms against infections. The phagocytic cup (see Fig. 1*B*) is an actin-based membrane structure formed at the plasma membrane of phagocytes, including macrophages, upon stimulation with foreign materials such as bacteria. The phagocytic cup captures and ingests foreign materials, and its formation is an essential first step in phagocytosis leading to the digestion of foreign materials (6, 7). When macrophages are stimulated by foreign materials, podosomes disappear, and phagocytic cups, which are also rich in F-actin, are formed to ingest the foreign materials (see Fig. 1*D*).

Wiskott-Aldrich syndrome (WAS) is an X chromosome-linked immunodeficiency disorder. Patients with WAS suffer from severe bleeding, eczema, recurrent infection, autoimmune diseases, and an increased risk of lymphoreticular malignancy (8–10). The causative gene underlying WAS encodes Wiskott-Aldrich syndrome protein (WASP) (11). WASP deficiency due to the mutation or deletion causes defects in adhesion, chemotaxis, phagocytosis, and the development of hematopoietic cells in WAS patients (10).

* This work was supported, in whole or in part, by National Institutes of Health Grant R01HD042752 (to S. T.). The costs of publication of this article were defrayed in part by the payment of page charges. This article must therefore be hereby marked "*advertisement*" in accordance with 18 U.S.C. Section 1734 solely to indicate this fact.

[S] The on-line version of this article (available at http://www.jbc.org) contains six supplemental figures.

[1] To whom correspondence should be addressed: Dept. of Biochemistry, Oyokyo Kidney Research Institute, 90 Yamazaki, Kozawa, Hirosaki 036-8243, Japan. Tel.: 81-172-87-1221; Fax: 81-172-87-1228; E-mail: tsuboi@oyokyo.jp.

[2] The abbreviations used are: M-CSF-1, macrophage-colony stimulating factor-1; FBP17, formin-binding protein 17; WAS, Wiskott-Aldrich syndrome; WASP, Wiskott-Aldrich syndrome protein; N-WASP, neuronal WASP; WIP, WASP interacting-protein; EFC domain, extended FER-CIP4 homology domain; F-BAR domain, FER-CIP4 homology and Bin-amphiphysin-Rvs domain; PMA, phorbol 12-myristate 13-acetate; GFP, green fluorescence protein; siRNA, short interfering RNA; FITC, fluorescein isothiocyanate; PDZ-GEF, PDZ-guanine nucleotide exchange factor; HEK293 cells, human embryonic kidney 293 cells; HA, hemagglutinin; SH3, src homology 3 domain; dSH3, SH3 domain deletion; GST, glutathione *S*-transferase; , $PI(4,5)P_2$, phosphatidylinositol 4,5-bisphosphate; siFBP, siRNA for FBP17; siC, scrambled control siRNA.